

# Temperature Dependence of the Deposition Behavior of Yttria-stabilized Zirconia CVD Films: Approach by Charged Cluster Model

In-Deok Jeon\*, Latifa Gueroudji\*\*, Doh-Yeon Kim\* and Nong-Moon Hwang\*\*\*†

\*Center for Microstructure Science of Materials, School Mater. Sci. & Eng. Seoul National University, Seoul 151-742, Korea

\*\*Korea Research Institute of Standards and Science, P.O. Box 102, Daejeon 305-600, Korea

(Received January 31, 2001, March 21, 2001)

## ABSTRACTS

Yttria-stabilized zirconia (YSZ) films were deposited with varying temperatures of  $ZrCl_4$  between 250~550°C with  $YCl_3$  and the substrate at 1000°C. Nanoamperes per square centimeter of the electric current were measured in the reactor during deposition and the current increased with increasing evaporation temperature of  $ZrCl_4$ . The zirconia nanometer size clusters were captured on the grid membrane near the substrate during the CVD process and observed by transmission electron microscopy (TEM). The deposition rate decreased with increasing evaporation temperature of  $ZrCl_4$ . A cauliflower-shaped structure was developed at 250°C then gradually changed to a faceted-grain structure above 350°C. Dependence of the growth rate and the morphological evolution on the evaporation temperature of  $ZrCl_4$  was approached by the charged cluster model.

**Key words:** YSZ,  $ZrO_2$ , CVD, Charged clusters, Current, Thin films

## 1. Introduction

In the chemical vapor deposition (CVD) process, the temperature dependence of the film growth rate is divided typically into three regions. The growth rate increases with increasing temperature in a certain temperature range and then above that range, the growth rate becomes relatively insensitive to the temperature increase and in some cases, the rate decreases with further increase of the temperature.<sup>1-5)</sup> This aspect is represented by the slopes in the plot of the logarithm of the growth rate against the inverse temperature. According to the standard classification,<sup>1-4)</sup> the higher slope in the lower temperature region indicates the surface reaction controlled growth and the lower slope in the higher temperature region indicates the gas-phase diffusion controlled growth. The negative slope in the high temperature range is attributed to the gas phase nucleation.<sup>1, 5)</sup>

Recently, however, Hwang et al.<sup>6, 7)</sup> suggested a charged cluster model (CCM) as the growth mechanism of thin films. According to the model, the gas phase nucleation occurs even when the supersaturation is so low as to achieve only a negligible film growth rate. In other words, under the conditions where the gas phase nucleation can be avoided, the film growth rate is negligible. This means that under practically meaningful processing conditions of thin films, the gas

phase nucleation occurs. Most of the gas phase nuclei are electrically charged so that their Brownian coagulation is inhibited and the nanometer size can be maintained during their residence time in the reactor. Besides, these charged nuclei are the major deposition flux for thin films. According to the CCM, the temperature dependence of the film growth rate is totally different from the classification based on the activation energy measurements. In the CCM, the temperature dependence of the film growth rate is related to the temperature dependence of cluster size, which is related to the supersaturation and the electric charge generation.

These hypothetical nuclei were experimentally confirmed in the diamond CVD,<sup>8, 9)</sup> the silicon CVD<sup>10)</sup> and thermal evaporation coatings of tungsten,<sup>11)</sup> gold<sup>12)</sup> and copper.<sup>13)</sup> Based on this new paradigm of growth mechanism, we could explain many puzzling phenomena occurring in the thin film process that could not be approached properly in the conventional concept of thin film growth by the atomic unit deposition. These phenomena include the low pressure synthesis of diamond,<sup>6, 14, 15)</sup> simultaneous deposition and etching of silicon,<sup>16, 17)</sup> selective deposition,<sup>17)</sup> the substrate effect on film morphology,<sup>18)</sup> growth of silicon nanowires<sup>19)</sup> and the electric bias effect on deposition.<sup>13)</sup>

The evolution of films by cluster deposition can be explained by the concept of the magic size suggested by Fujita.<sup>20-22)</sup> Fujita found out that the transition between fast-diffusion liquid-like and slow-diffusion crystalline properties takes place abruptly with size of the clusters, which he called a magic size. He determined the magic size for an

†Corresponding author : nmhwang@kriss.re.kr

embedded  $ZrO_2$  cluster to be ~6 nm at room temperature.<sup>21)</sup> The magic size for the isolated state is expected to be ~12 nm. When clusters are smaller than the magic size, clusters will make epitaxial landing on the growing surface. When they are larger than the magic size, they tend to retain their individual orientations, leading to a nanostructure or cauliflower structure. This microstructure transition takes place relatively abruptly with the cluster size. These aspects of cluster deposition were revealed also by molecular dynamic simulation in gold cluster deposition.<sup>23)</sup>

Therefore, many features of thin films, which had been approached by the conventional concept of atomic unit deposition, should be reexamined. Among these, the temperature dependence of the deposition behavior will be approached by the CCM in this paper with a focus on the yttria stabilized zirconia (YSZ) CVD. The generation of nanometer-size clusters in the gas phase during the typical CVD process was revealed in the nanometer-size powder synthesis by chemical vapor condensation method,<sup>24)</sup> where powders or films of SiC,  $Si_3N_4$ ,  $Al_2O_3$ ,  $TiO_2$ ,  $ZrO_2$  and other refractory compounds were synthesized. Nevertheless, in this paper we tried to confirm the generation of charged zirconia nuclei in two ways. One is by measuring the electric current during the thermal evaporation of  $ZrCl_4$ , which is an indirect indication of charged zirconia nuclei because ionization of a single atom or molecule is negligible at the temperature used in the CVD process. The other is by capturing the clusters on the grid membrane and observing them by transmission electron microscopy (TEM). Since the amount of electric current or the charge density is related to the cluster size, which plays a critical role in the microstructure evolution of the film, the growth rate of the film and the morphology with varying evaporation temperature of  $ZrCl_4$  precursor could be approached from a viewpoint of CCM.

## 2. Experimental Procedure

A 3-zone tube furnace was used for CVD of  $ZrO_2$ . The schematic diagram of the thermal CVD reactor was

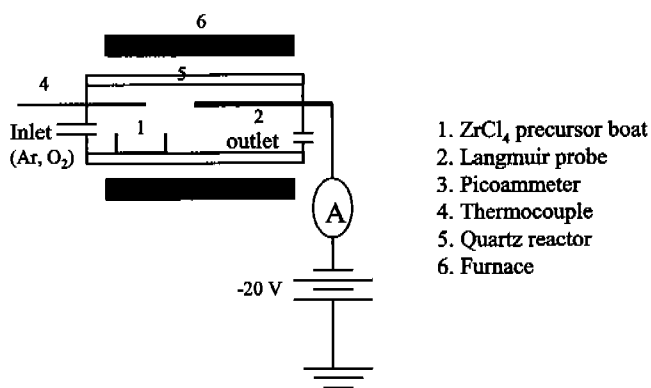


Fig. 1. Schematic diagram for measurement of the current inside the CVD reactor by a Faraday cup.

reported previously.<sup>25)</sup> In order to check the generation of electric charge during deposition in the reactor, the current was measured by a Faraday cup as shown in Fig. 1 with varying evaporation temperature of the  $ZrCl_4$  (99.9%, Aldrich) precursor. Negative bias of -20 V was applied for repelling electrons. The current was measured at two locations in the reactor: one is near the precursor and the other on the substrate position. In the first case, the temperature was ~100°C higher than that of the  $ZrO_2$  precursor and in the second case, the temperature was fixed at 1000°C. Platinum wire was used for the probe due to its high conductivity and the inertness for chlorine. The collecting area of the platinum wire was ~50 mm<sup>2</sup>. Keithly 416 Pico ammeter was used.

For deposition,  $ZrCl_4$  (99.9%, Aldrich) and  $YCl_3$  (99.9%, Aldrich) powders were used as precursors and oxygen was used as a reactive gas. The temperatures of substrates and  $YCl_3$  were controlled within ±5°C and that of  $ZrCl_4$  was within ±20°C.  $ZrCl_4$  was heated to 250~550°C and  $YCl_3$  was to 1000°C. The deposition was done for 2 hrs.  $YCl_3$  precursor and the substrate were placed at the site of the same temperature.

In order to capture the individual YSZ nuclei from the gas phase, the Ni grid with a silica membrane for TEM was attached to a liquid-nitrogen cooled cold finger made of stainless steel and exposed near the substrate for 60 sec at the  $ZrCl_4$  evaporation temperature of 250°C. The captured clusters were observed by TEM (Hitachi, H-9000NAR). The growth rate of the films was estimated by scanning electron microscopy (SEM, Akashi ISI DS-130C) of cross-section of the YSZ films. The  $Y_2O_3$  fraction in the films was determined by electron probe microanalyzer (EPMA, Cameca SX-50). SEM was used for observing microstructures.

## 3. Results

### 3.1 Generation of electric charge in the reactor

The current generation with the evaporation temperature

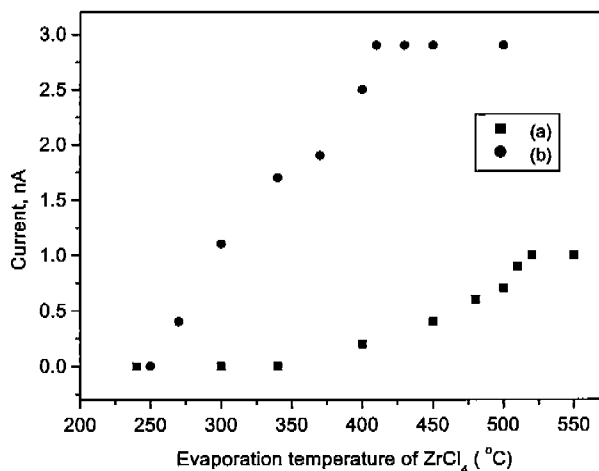


Fig. 2. Current produced (a) near the evaporation temperature of  $ZrCl_4$  and (b) at the location for the film deposition.

of the  $ZrCl_4$  precursor is shown in Fig. 2(a). Here, the temperature for current measurements was about  $100^\circ\text{C}$  higher than the precursor temperature. The current increased relatively steeply in the temperature range of  $300\sim 400^\circ\text{C}$  and nearly saturated at  $\sim 550^\circ\text{C}$  as  $\sim 1$  nA. The collecting area for current was  $\sim 50$  mm<sup>2</sup> so that the current density is  $\sim 2$  nA/cm<sup>2</sup>. Since the amount of current can be different between the temperatures of precursor evaporation and film deposition, we also measured the current at the location of the substrate as a function of temperature of the  $ZrCl_4$  precursor as shown in Fig. 2(b). The current, compared with that of Fig. 2(a), increased about 3 times and increased abruptly at  $\sim 300^\circ\text{C}$  and saturated at  $\sim 450^\circ\text{C}$  of the  $ZrO_2$  precursor. These temperatures are  $50\sim 100^\circ\text{C}$  lowered than those of Fig. 2(a).

### 3.2 Growth rate of the film with the $ZrCl_4$ temperature

The growth rate of the film was  $\sim 1$   $\mu\text{m/hr}$  in the  $450\sim 550^\circ\text{C}$  of  $ZrCl_4$  temperature, which corresponds to the range that the current is saturated as shown in Fig. 2. The growth rates were  $\sim 10$  and  $\sim 5$   $\mu\text{m/hr}$ , respectively, at the  $ZrCl_4$  temperatures of  $250$  and  $350^\circ\text{C}$ . These results indicate that the growth rate of the film decreased with

increasing evaporation temperature of  $ZrCl_4$  in this temperature range. This aspect is unusual because the high deposition rate is expected from the high evaporation rate. Below  $250^\circ\text{C}$  of the  $ZrCl_4$  precursor, the growth rate decreased with decreasing evaporation temperature of  $ZrCl_4$ .

The dependence of the  $ZrO_2$  growth rate on the evaporation temperature of  $ZrCl_4$  can also be indirectly estimated by the relative fraction between  $ZrO_2$  and  $Y_2O_3$  in the film because the evaporation temperature of  $YCl_3$  was fixed. The  $Y_2O_3$  fractions in the film increased from 2 to 25% as the  $ZrCl_4$  temperature increased from  $250$  to  $550^\circ\text{C}$ . These results indicate that the growth rate of  $ZrO_2$  decreased with increasing evaporation temperature of  $ZrCl_4$  in agreement with the growth rate measured by SEM.

### 3.3 Microstructure of films

Fig. 3 shows the zirconia clusters observed by TEM. The cluster size was  $\sim 8$  nm. The high resolution image of Fig. 3(b) shows the lattice fringe of zirconia clusters. The agglomeration behavior of clusters shown in Fig. 3(a) indicates that these clusters were not formed on the substrate but landed from the gas phase.

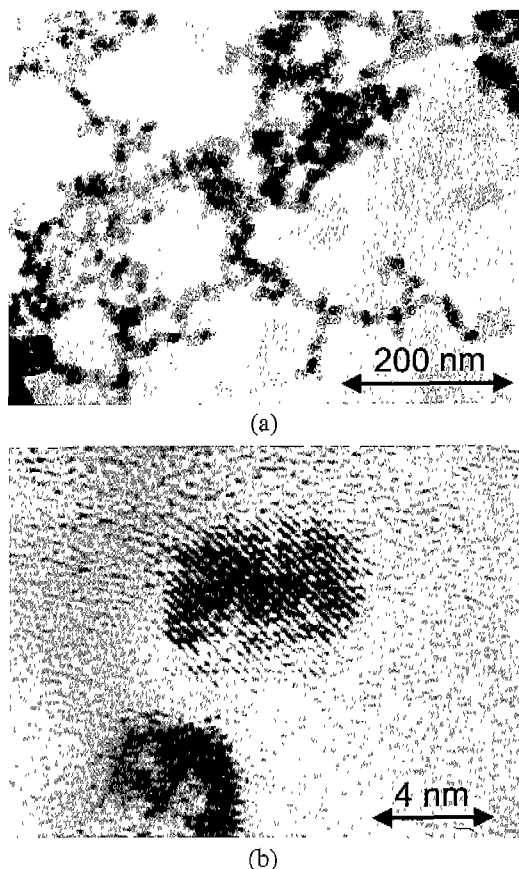


Fig. 3. TEM of (a) lower and (b) higher magnifications of the YSZ nuclei captured for 60 sec on a grid membrane at the cold finger near the substrate at the  $ZrCl_4$  evaporation temperature of  $250^\circ\text{C}$ .

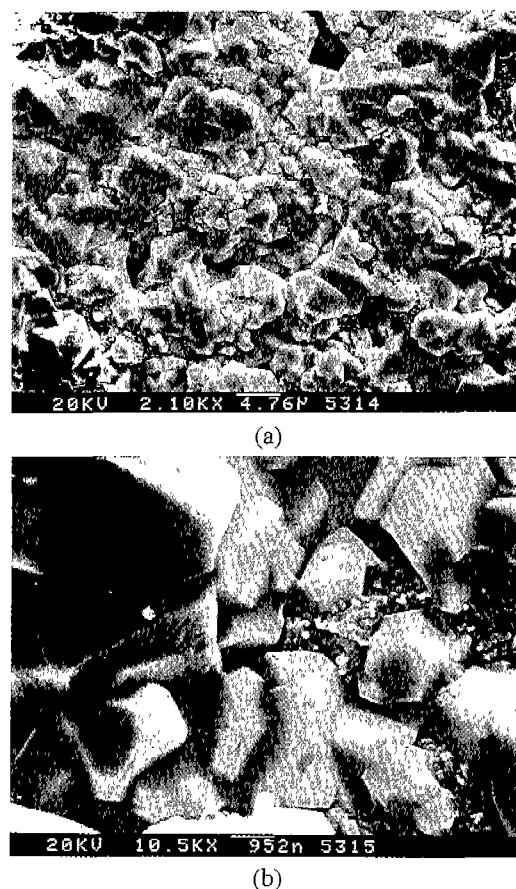
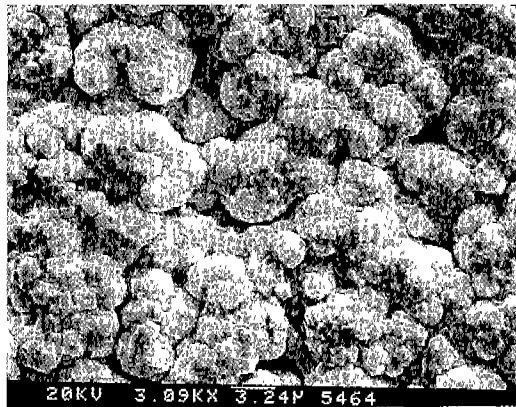
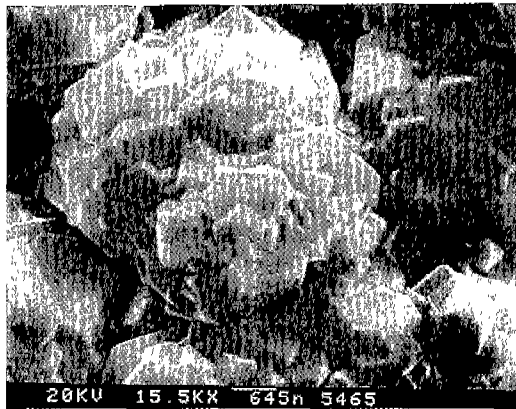


Fig. 4. SEM of (a) lower and (b) higher magnifications of the YSZ film deposited for 2 hrs at  $T_{ZrCl_4}=400^\circ\text{C}$ ,  $T_{YCl_3}=1000^\circ\text{C}$  and  $T_{\text{sub}}=1000^\circ\text{C}$ .



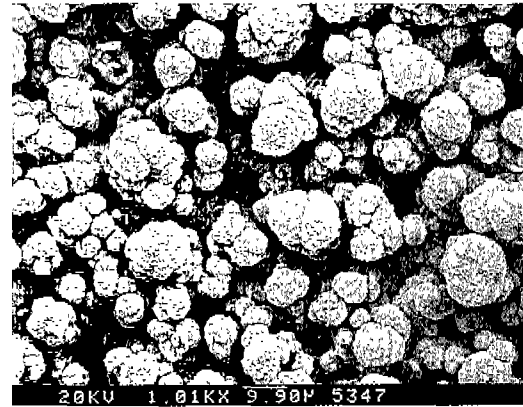
(a)



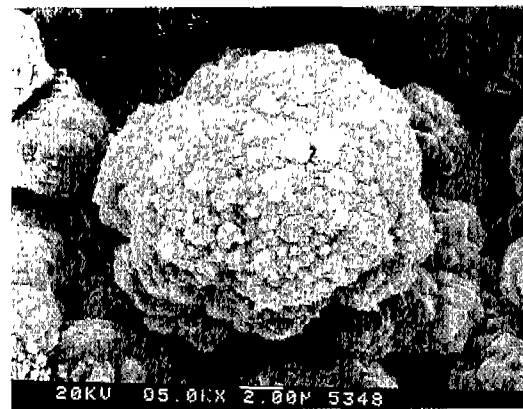
(b)

Fig. 5. SEM of (a) lower and (b) higher magnifications of the YSZ film deposited for 2 hrs at  $T_{\text{ZrCl}_4}=345^\circ\text{C}$ ,  $T_{\text{VCl}_3}=1000^\circ\text{C}$  and  $T_{\text{sub}}=1000^\circ\text{C}$ .

Figs 4, 5 and 6 show the variations of microstructures for three different  $\text{ZrCl}_4$  temperatures of 450, 350 and 250°C, respectively. SEM photographs of both lower and higher magnifications were shown in each case. The films with well-developed facets with grain size of  $\sim 3$   $\mu\text{m}$  tended to develop at the evaporation temperature of 450°C of the  $\text{ZrCl}_4$  precursor (Fig. 4) while the film morphology resembling the cauliflower tended to develop at 250°C of the  $\text{ZrCl}_4$  precursor (Fig. 6). In the medium temperature of 350°C (Fig. 5), the microstructure shows the transition from faceted to cauliflower-shaped structures with grain size of  $\sim 0.5$   $\mu\text{m}$ . At 250°C of  $\text{ZrCl}_4$ , grains with well-developed facets appeared no more. While each grain of  $\sim 3$   $\mu\text{m}$  in Fig. 4 is single crystalline, each spherical lump of  $\sim 5$   $\mu\text{m}$  in Fig. 6 is polycrystalline consisting of numerous tiny submicron grains. The growth rate of the cauliflower-shaped films in Fig. 6 was 5~10 times higher than that of the films with well-developed facets in Fig. 4. In the  $\text{ZrCl}_4$  temperature range of 300~400°C, the microstructure changed from being cauliflower-shaped to being faceted. This temperature range corresponds to the abrupt current increase in the reactor chamber (Fig. 2).



(a)



(b)

Fig. 6. SEM of (a) lower and (b) higher magnifications of the YSZ film deposited for 2 hrs at  $T_{\text{ZrCl}_4}=250^\circ\text{C}$ ,  $T_{\text{VCl}_3}=1000^\circ\text{C}$  and  $T_{\text{sub}}=1000^\circ\text{C}$ .

#### 4. Discussion

Fig. 2 shows that the electric charge is generated during evaporation of  $\text{ZrCl}_4$  precursor. In Fig. 2(a), the current increased with increasing temperature of  $\text{ZrCl}_4$ . This result indicates that the generation of charge increased with increasing flux of precursor evaporation. Although the current in Fig. 2 is small compared to that measured in the hot filament or the plasma CVD process, it is comparable to the current measured during the silicon thermal CVD process<sup>17)</sup> and the thin film deposition by gold evaporation in the tungsten basket at 1250°C.<sup>12)</sup> The ionization energy of the involved species is too high to generate such a high current at the temperature of the reactor. The current measured in Fig. 2 can only be explained by the surface ionization of the nuclei, as analyzed previously in thermal evaporation of metals.<sup>13)</sup> The ionization energy of nuclei is close to the work function of the bulk. As a result, the activation energy for the surface ionization of these nuclei can be less than  $\sim 1$  eV, which can explain the current generation of Fig. 2. Therefore, the generation of electric current shown in Fig. 2 is the indication of gas phase nucleation of zirconia.

It is known that the agglomerated clusters in Fig. 3(a) can

be prepared in the non-agglomerated state when they are quenched into the liquid nitrogen cooled drum and scrapped.<sup>24)</sup> Besides, when the substrate was placed in the presence these clusters, the dense films were developed.<sup>24)</sup> This aspect is also shown in Figs. 4, 5 and 6.

Measurements of the film thickness in the cross section by SEM observation showed that the growth rate of the film decreased with increasing evaporation temperature of  $ZrCl_4$ . The same behavior was also revealed by the increase of the  $Y_2O_3$  fraction in the film with increasing temperature of  $ZrCl_4$ . This behavior is difficult to understand because the higher evaporation temperature of  $ZrCl_4$  corresponds to the higher flux of  $ZrO_2$ . Besides, the low growth rate at a high temperature tends to be accompanied by large grains with well-developed facets (Fig. 4) while the high growth rate at a low temperature tends to be accompanied by a cauliflower-shaped structure (Fig. 6).

Decrease in the growth rate with increasing processing temperature is quite a common phenomenon in the CVD process.<sup>1,5)</sup> According to the conventional explanation, the gas phase nucleation occurs at a high temperature while it is suppressed at a low temperature.<sup>1,5)</sup> Since the gas phase nucleation decreases the supersaturation markedly, the growth rate is low and the grains are large with well-developed facets at a high temperature.

According to the CCM, however, the gas phase nucleation occurs at low temperatures as well as at high temperatures, as supported by the current measurements shown in Fig. 2 and by TEM observation of individual zirconia clusters in Fig. 3. In the CCM, the cluster size is the most important factor affecting the deposition behavior. The cluster size depends on the nucleation rate, which again depends on the supersaturation. If the supersaturation is high, the nucleation rate will be high and as a result, the size of the nuclei will be small. Since each nucleus tends to be electrically charged when they grow above a certain size, the high nucleation rate will increase the generation of charge or current, which explains the dependence of the current on the evaporation temperature of  $ZrCl_4$  in Fig. 2.

Therefore, the high current at the high evaporation temperature of  $ZrCl_4$  in Fig. 2 is an indication of the small cluster size. Since the small clusters have the liquid-like property in diffusion,<sup>20,23)</sup> they tend to undergo epitaxial recrystallization after landing, resulting in large grains with well-developed facet. On the other hand, the large clusters do not have the liquid-like property and tend to fail frequently in epitaxial recrystallization. Each failure of epitaxial recrystallization will make twin or grain boundaries, leading to the formation of secondary nuclei. In the extreme case of large clusters, each cluster will be the individual grain of the final film, resulting in a nanostructure. Therefore, as the cluster size increases, the frequency of epitaxial recrystallization will decrease and the grain size of the film will decrease with the microstructure changing from the large faceted grains in Fig. 4 to the cauliflower-shaped grains in Fig. 6.

According to the study of the deposition behavior of clusters by molecular dynamics,<sup>23)</sup> it took a much shorter time for the cluster to complete epitaxial recrystallization than for the cluster to take a shape of surface energy minimization into a two dimensional disc. In other words, the rate of the surface diffusion was much slower than the rate of epitaxial recrystallization. Thus, even if the clusters deposit epitaxially, the surface morphology of the film can be macroscopically rough. Thus, the grain size of the cauliflower-shaped structure need not be one tiny nodule but the actual grain size can be much larger or can have a columnar structure.

The cluster size also affects the growth rate of the film especially when the charged clusters are not a good conductor because the Coulomb repulsion tends to be diminished for the large clusters. The higher film growth rate can be provided by the larger clusters, which are generated at the low evaporation temperature of  $ZrCl_4$ . Considering the temperature dependence of the vapor pressure of  $ZrCl_4$ , the total cluster flux must be much larger at the higher evaporation temperature. Unless the Coulomb repulsion between the clusters and the growing surface is the rate-limiting step in film growth, the high evaporation temperature should provide a high growth rate. In the temperature range where the film growth rate decreases with increasing temperature, the Coulomb repulsion would be the rate-limiting step in film growth and the large clusters have an advantage over the small ones in the film growth rate.

We suggested that the nanostructure or cauliflower structure could be one of the microstructure criteria that distinguish between the atomic unit and the cluster unit deposition.<sup>7)</sup> Since this problem is critical in this paper and the evolution of a cauliflower structure is quite common in many thin film processes, it will be treated in more detail. For the evolution of a cauliflower structure in Fig. 6 by an atomic or a molecular unit, the secondary nucleation should occur on the growing surface. The barrier of secondary nucleation is higher than that of growth because of the excess interface free energy between the growing surface and the nucleus. The maximum barrier for growth is 2-dimensional nucleation (2-DN). How much the given grain can grow before another secondary nucleation will determine the grain size. Thus, the grain size will be determined by the ratio of the secondary nucleation rate and the 2-DN rate. Previously, Hirth and Pound<sup>26)</sup> estimated this ratio to be  $\sim 10^{13}$ . This means that one secondary nucleation with an incoherent boundary takes place after growth of  $\sim 10^{13}$  atomic layers by 2-DN. Therefore, the minimum grain size should be a few centimeters. The evolution of a nanostructure or a cauliflower structure is difficult to explain by an atomic or a molecular unit. Therefore, it is more likely that the nanostructure is formed by landing of nano particles formed in the gas phase as suggested in the CCM.<sup>6,7)</sup>

On the other hand, quite often in the other CVD process,

the cauliflower structure changed to the crystal with well-defined facets with the marked decrease in the growth rate when the substrate temperature increases above some values.<sup>27)</sup> Although the low growth rate has been attributed to the onset of the gas phase nucleation,<sup>1, 5, 28)</sup> such transition in the deposition behavior with increasing substrate temperature might be attributed to the increase in the charge density as in the case of our present experiment. In this high temperature condition, the cluster size is small and favorable for epitaxial growth. This aspect is in agreement with the actual process for epitaxial growth, which adopts the high temperatures.<sup>5)</sup>

## 5. Conclusion

Individual zirconia clusters were observed by TEM after capturing them on a grid membrane. Besides, the electric current was generated with evaporation of  $ZrCl_4$  precursor. It increased with increasing evaporation temperature of  $ZrCl_4$ . The decreasing deposition rate with increasing evaporating temperature of  $ZrCl_4$  in the range of 250~550°C could be explained by the CCM. The transition from the cauliflower-shaped structure to the structure with well-defined facets with increasing temperature could also be explained by the CCM.

## Acknowledgment

This work was supported by Creative Research Initiatives Program of Korea Ministry of Science and Technology.

## REFERENCES

1. C.F. Powell, J.H. Oxley and Jr. J.M. Blocher, "Vapor Deposition," in *Ch 1. Vapor-Deposited Materials*, edited by Jr. J.M. Blocher (John Wiley & Sons, Inc., New York, 1966), pp. 3-22.
2. J.L. Vossen and W. Kern, "Thin Film Process," in *Chemical Vapor Deposition of Inorganic Thin Films* edited by W. Kern and V.S. Ban (Academic Press, New York, 1978), pp. 257-331.
3. D.W. Shaw, "Mass Transport-Type II or Diffusion Control in Crystal Growth, Theory & Techniques (Plenum, New York, 1974).
4. A. Matthews and D.S. Rickerby, "Thermally Activated Chemical Vapor Deposition" in *Advanced Surface Coating: A Handbook of Surface Engineering* (Chapman and Hall, New York, 1991).
5. C.E. Morosanu, *Thin Films by Chemical Vapour Deposition* (Elsevier, Amsterdam, 1990).
6. N.M. Hwang, J.H. Hahn and D.Y. Yoon, "Charged Cluster Model in the Low Pressure Synthesis of Diamond," *J. Crystal Growth*, **162**, 55-68 (1996).
7. N.M. Hwang, "Crystal Growth by Charged Cluster: Focused on CVD Diamond," *J. Crystal Growth*, 198/199, 945-950 (1999).
8. I.D. Jeon, C.J. Park, D.Y. Kim and N.M. Hwang, "Experimental Confirmation of Charged Carbon Clusters in the Hot Filament Diamond Reactor," *J. Crystal Growth*, **213**, 79-82 (2000).
9. I.D. Jeon, C.J. Park, D.Y. Kim and N.M. Hwang, "Effect of Methane Concentration on Size of Charged Clusters in the Hot Filament Diamond CVD Process," *J. Crystal Growth*, **223**, 6-14 (2001).
10. W.S. Cheong, N.M. Hwang and D.Y. Yoon, "Observation of Nanometer Silicon Clusters in the Hot-Filament CVD Process," *J. Crystal Growth*, **204**, 52-61 (1999).
11. K.S. Seo, "Study on the Mechanism of Tungsten Thin Film Prepared by Evaporation," MS, Chunbuk Univ., 1998.
12. M.C. Barnes, D.Y. Kim, H.S. Ahn, C.O. Lee and N.M. Hwang, "Deposition Mechanism of Gold by Thermal Evaporation: Approach by Charged Cluster Model," *J. Crystal Growth*, **213**, 83-92 (2000).
13. B.S. Lee, "Spontaneous Formation of Charged Clusters during Thermal Evaporation of Metals," MS Thesis, Seoul National University, 2000.
14. N.M. Hwang, J.H. Hahn and D.Y. Yoon, "Chemical Potential of Carbon in the Low Pressure Synthesis of Diamond," *J. Crystal Growth*, **160**, 87-97 (1996).
15. N.M. Hwang and D.Y. Yoon, "Thermodynamic Approach to the Paradox of Diamond Formation with Simultaneous Graphite Etching in the Low Pressure Synthesis of Diamond," *J. Crystal Growth*, **160**, 98-103 (1996).
16. N.M. Hwang, "Deposition and Simultaneous Etching of Si in the CVD Process: Approach by the Charged Cluster Model," *J. Crystal Growth*, **205**, 59-63 (1999).
17. N.M. Hwang, W.S. Cheong and D.Y. Yoon, "Deposition Behaviors of Si on Insulating and Conducting Substrates in the CVD Process: Approach by Charged Cluster Model," *J. Crystal Growth*, **206**, 177-86 (1999).
18. W.S. Cheong, D.Y. Yoon, D.Y. Kim and N.M. Hwang, "Effect of Substrates on Morphological Evolution of a Film in the Silicon CVD Process: Approach by Charged Cluster Model," *J. Crystal Growth*, **218**, 27-32 (2000).
19. N.M. Hwang, W.S. Cheong, D.Y. Yoon and D.Y. Kim, "Growth of Silicon Nanowires by Chemical Vapor Deposition: Approach by Charged Cluster Model," *J. Crystal Growth*, **218**, 33-39 (2000).
20. H. Fujita, "Usefulness and Applications of Electron Microscopy to Materials Science," *Mater. Trans. JIM* **31**(7), 523-37 (1990).
21. H. Fujita, "Atom Clusters - New Applications of High-Voltage Electron Microscopy "Micro-Laboratory" to Materials Science," *Ultramicroscopy* **39**, 369-381 (1991).
22. H. Fujita, "Studies on Atom Clusters by Ultra-High Voltage Electron Microscopy," *Mater. Trans., JIM* **35**(9), 563-75 (1994).
23. S.-C. Lee, N. M. Hwang, B. D. Yu and D.Y. Kim, "Molecular Dynamics Simulation on the Deposition Behavior of Nanometer-Sized Au Clusters on a Au(001) Surface," *J. Crystal Growth*, **223**, 311-20 (2001).
24. Y. Chen, N. Glumac, B.H. Kear and G. Skandan, "High Rate Synthesis of Nanophase Materials," *NanoStructured Materials* **9**, 101-04 (1997).
25. I.D. Jeon, L. Gueroudji and N.M. Hwang, "Deposition of Yttria Stabilized Zirconia by the Thermal CVD Process,"

- Kor. J. Ceram.*, **5**, 131-36 (1999).
26. J.P. Hirth and G.M. Pound, *Condensation and Evaporation* (Pergamon Press, Oxford, 1963).
27. L. Ben-Dor, A. Elshtein, S. Halashi, I. Pinshky and J. Shapir, "Thin Films of  $ZrO_2$  Metal Organic Chemical Vapor Deposition," *J. Electronic Materials*, **13**(2), 263-72 (1984).
28. E.T. Kim and S.G. Yoon, "Characterization of Zirconium Dioxide Film Formed by Plasma-Enhanced Metall-Organic Chemical Vapor Deposition," *Thin Solid Film*, **227**, 7-12 (1993).